Spectrum of Mechanical Engineering and Operational Research

Journal homepage: www.smeor-journal.org
eISSN: 3042-0288

Effect of Repetitive High-Density Current Pulses on Plastic Deformation of Copper Wires under Stepwise Loading

Sergey V. Dmitriev[1,2,*], Alina Y. Morkina[3,4], Danila V. Tarov[4], Gulnara R. Khalikova[3,5], Dina U. Abdullina[1], Pavel S. Tatarinov[6], Vladimir P. Tatarinov[6], Alexander S. Semenov[6], Oleg B. Naimark[7], Andrey V. Khokhlov[8], Vladimir V. Stolyarov[9]

1 Institute of Molecule and Crystal Physics, UFRC of Russian Academy of Sciences, Ufa, Russia
2 Department of Equipment and Technologies of Welding and Control, Ufa State Petroleum Technological University, Ufa, Russia
3 Institute for Metals Superplasticity Problemsof Russian Academy of Sciences, Ufa, Russia
4 Research Laboratory for Metals and Alloys under Extreme Impacts, Ufa University of Science and Technology, Ufa, Russia
5 Department of Technological Machines and Equipment, Ufa State Petroleum Technological University, Ufa, Russia
6 Polytechnic Institute (Branch) in Mirny, North-Eastern Federal University, Mirny, Sakha Republic (Yakutia), Russia
7 Institute of Continuous Media Mechanics of the Ural Branch of Russian Academy of Sciences, Perm, Russia
8 Institute of Mechanics, Lomonosov Moscow State University, Moscow, Russia
9 Mechanical Engineering Research Institute of Russian Academy of Sciences, Moscow, Russia

ARTICLE INFO

Article history:
Received 12 February 2024
Received in revised form 22 April 2024
Accepted 17 May 2024
Available online 22 May 2024

Keywords:
Electroplastic Effect; Creep; Current Pulses; Copper; Tensile Deformation.

ABSTRACT

High-density electric current pulses increase the plasticity and reduce the yield stress of metals with negligible heat generation. This effect has great potential for the development of energy-saving technologies for processing hard-to-deform metallic materials. Despite the long history of the study of electroplasticity, there is still no consensus on the physical nature of this effect. In this paper, the effect of repetitive pulses applied at the same or gradually increasing tensile stress on the plastic deformation of copper wire is investigated using a home-made experimental setup. The electroplasticity of the wire in the delivery state and after annealing is compared. It is shown that for a constant tensile stress, the incremental plastic deformation of the wire decreases with each successive pulse. This effect is stronger for annealed wires because they have a lower dislocation density and therefore a lower plasticity resource. The Joule heat release in the specimen and the heating due to plastic deformation are evaluated. The results obtained will be used to fit the parameters of the atomistic model being developed to describe the interaction of electron flow with dislocations.

1. Introduction

The electroplastic effect (EPE) in metals was discovered by Troitskii in 1969 [1] and later investigated in a number of seminal studies [2]. The effect is a decrease in the yield stress of metallic materials when current pulses are passed through them. Notably, the temperature

* *Corresponding author.*
E-mail address: dmitriev.sergey.v@gmail.com

https://doi.org/10.31181/smeor1120243

increase of the deformed material can be small, and Joule heating alone cannot explain the significant increase in plasticity. As a result, energy costs for forming parts can be saved compared to traditional methods of processing materials by pressure. In recent years, research on EPE has become increasingly popular [3-6] since this effect has found applications in various industries. Due to the skin effect [7], a non-thermal reduction in flow stress can be observed in relatively thin workpieces in such manufacturing processes as drawing [8,9], rolling [10,11], stamping [12], forging [13,14], cutting [15], and forming [5,6,16-19].

Despite the widespread use of EPE, the underlying principles are still unclear. According to many studies, the two main mechanisms explaining this effect are the non-homogeneous release of Joule heat and the electron wind [20-22]. The heat released at the defects, such as dislocations and grain boundaries, increases their mobility and enhances plasticity; the average temperature increase remains insignificant. The electron wind exerts a force on the dislocations that also increases their mobility. There are experimental works reporting data in favor of the electron wind theory [22]. On the other hand, in [23] a non-directional migration of the twin boundary upon electropulsing was observed and interpreted as being governed by the electron-dislocation interaction rather than the electron wind force. In order to clarify the effect of Joule heat, the paper [24] compared an asynchronous loading with a high energy current with a synchronous loading with a low energy current. The mechanisms of electro-mechanical coupling were discussed in the reviews [25-27].

Recently, a number of works have been carried out to better understand EPE and to apply it to the processing of various metallic materials. A method for self-healing of metallic materials based on microstructure restoration using pulsed electric current has been proposed by Jeong et al [28]. In the work of Kim et al. [29], it was shown that passing an electric current during the tensile testing of an Al-Mg-Si alloy can promote annealing, aging and void formation during tensile testing. The possibility of improving the ductility of a Mg-Nd-Zn-Zr alloy was demonstrated in [30]. The effect of strain rate on plasticity and microstructure for the electrically assisted tension of the 5754-H111 aluminum alloy was analyzed in [31]. Mechanisms of electroplasticity in hcp metals were studied in [32,33]. The effect of microstructure on EPE in AA 6063 alloy was addressed in [34]. Precipitation hardening of high-strength steel induced by electric current has been analyzed in [35]. EPE in a high-temperature strength nickel-chromium-tungsten-molybdenum Haynes 230 alloy was explored in [36]. The effect of temperature on EPE in the Invar 36 alloy was investigated in [37]. The effect of angle between direction of load and electric pulse current on EPE in Ti-6Al-4V alloy was analyzed in [38]. EPE in a high entropy alloy subjected to uniaxial tension was studied in [39], where the decrease in yield stress and the increase in elongation with increasing current density were observed. Enhanced plasticity due to electric pulses was reported in [40] for monatomic metallic glasses. The motion of individual dislocations as a result of combined electromechanical actuation was studied *in situ* in single crystal nickel [41] and copper [42].

Electrical pulses can be used not only to increase the plasticity of metals, but also to influence the defect structure in metals [43,44], to heal fatigue cracks [45,46], to increase wear and corrosion resistance [47,48], and for joining dissimilar metals [49].

Electroplasticity was studied for different loading schemes, e.g., during bending [50], compression [51], tension [52-55], and nanoindentation [56]. If the deformation increment decreases with the pulse number at constant stress then this is in favor of the fact that electroplasticity is not only due to the Joule heating but also due to the dislocation de-pinning. This was found in the work [56] for electric pulse assisted nanoindentation and macroscopic compression.

The purpose of this study is to analyze the effect of several high-density electric current pulses on the deformation of copper samples in different structural states under tension produced by the dead load. The temperature of the specimens after passing the electric current pulse is estimated. Thermal energy release due to plastic deformation of the wire is calculated.

2. Material and Methodology

2.1 Microstructure Characterization

In this work, Cu-ETP M1 grade copper wire with the chemical composition shown in Table 1 is used. This material is chosen because it is used for massive wire production and wire drawing can be more efficient using electrical pulses [57,58]. The specimens, 360 mm in length, were cut from 1 mm diameter copper wire. Two structural states are considered, as-received and annealed at a temperature of 500°C for 2 hours and cooled with a furnace.

Table 1
Chemical composition of grade M1 copper

Mass fraction of element										
Cu	Impurities, no more									
no less	Bi	Fe	Ni	Zn	Sn	Sb	As	Pb	S	O
99.90	0.001	0.005	0.002	0.004	0.002	0.002	0.002	0.005	0.004	0.05

In order to characterize the microstructure of the copper wires, the electron backscatter diffraction (EBSD) analysis was performed. The surface of the specimens for EBSD analysis was prepared as follows: material blanks were cut into plates using an electric spark method, then these plates were thinned mechanically on sanding paper with a gradual decrease in the abrasive value, after which they were polished using diamond paste, also with a sequential transition to a finer abrasive. The final polishing was carried out by jet electropolishing on a Tenupol – 3 apparatus using a 20% aqueous solution of H_3PO_4. EBSD analysis was carried out on a TESCAN MIRA scanning electron microscope at an accelerating voltage of 20 kV. Statistical analysis of the data, including estimation of the average grain size, was carried out using the built-in software package "CHANNEL 5.0" at a confidence level of 95%. EBSD maps were obtained with a scanning step of 0.5 μm, the maximum permissible error in determining the orientation was 2°. To improve the reliability of the obtained EBSD data using a method proposed by Humphreys [59], fine grains containing 5 or fewer pixels were automatically "cleaned up" using the standard grain expansion option of the EBSD software.

EBSD images of the microstructure and misorientation angle distributions are shown in Figure 1 for the as-received sample and Figure 2 for the annealed sample. The left and right columns of these figures show the results for the cross sections along the wire axis and perpendicular to the wire axis, respectively. In panels (a) and (b), the grain orientation maps are shown according to the color legend. In (c) and (d), the grain boundary maps showing the low angle boundaries (LABs) with $2°<\Theta<15°$ and high angle boundaries (HABs) with $\Theta\geq15°$ are shown by red and black lines, respectively (Θ is the misorientation angle). The twin boundaries (TBs) are also indicated by green lines. In (e) and (f) the distribution of grain boundaries over misorientation angles is shown.

Comparing panels (a) and (b) in Figure 1, it can be seen that the orientation of the grains in the as-received structure is random in the longitudinal direction, but in the transverse direction they have predominant orientations close to <001> and <111> (red and blue colors of grains, respectively). A large proportion of twin boundaries are observed in the structure, see green lines in Figure 1(c) and (d). Most of the grain boundaries have a high angle of misorientation. The average grain size, excluding twin boundaries, is 9.1 ± 0.4 μm and 8.2 ± 0.2 μm in the longitudinal and transverse directions, respectively. After annealing, see Figure 2, the copper structure recrystallizes and the average grain size increases to 113.8 ± 20.7 μm and 50.4 ± 8.9 μm in the longitudinal and transverse directions, respectively. The predominant orientation of grains near <001> and <111> and the presence of a large proportion of twin boundaries remain after annealing.

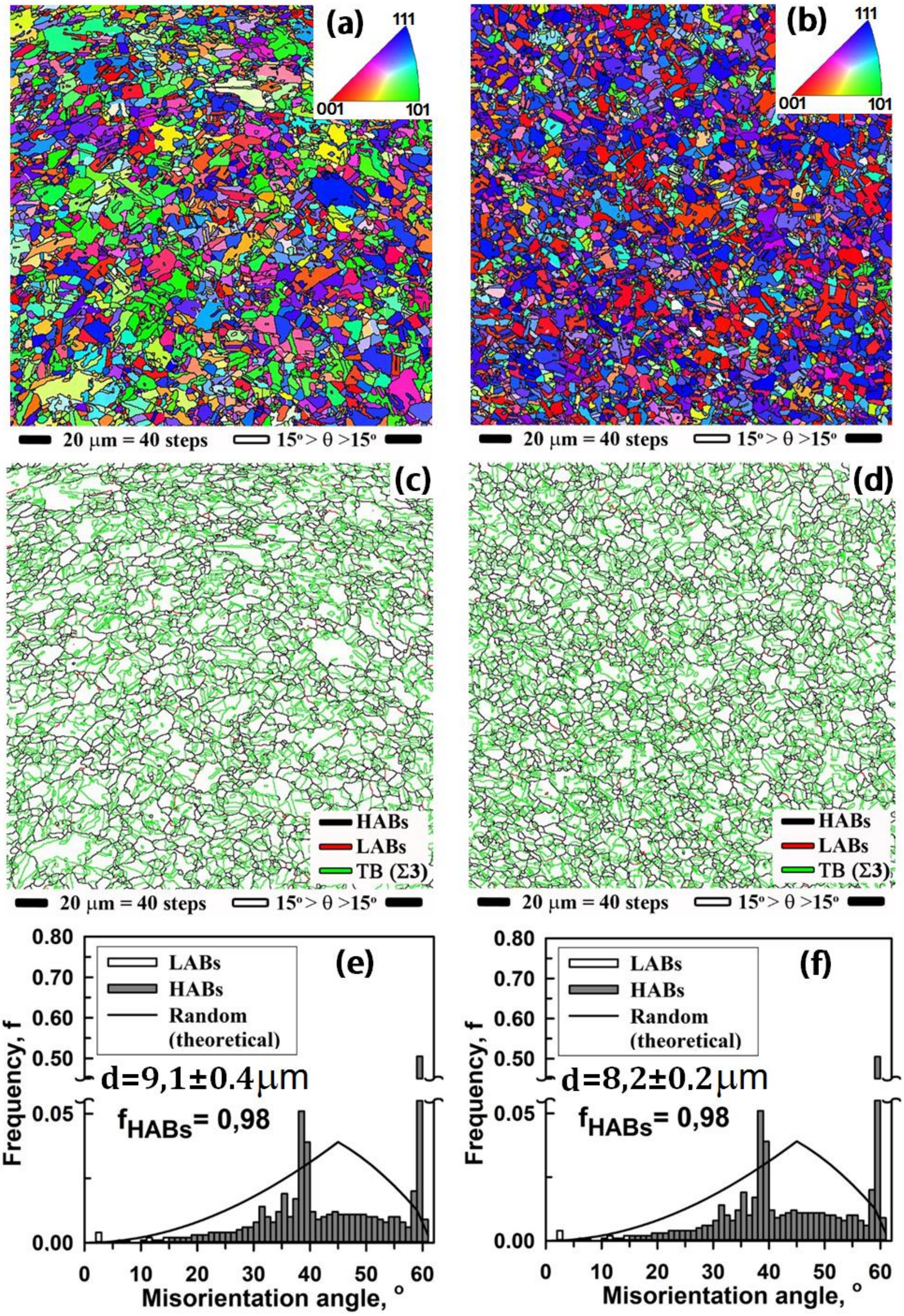

Fig. 1. The microstructure of the as-received copper wire. (a,b) Grain orientation distribution maps. (c,d) Grain boundary distribution maps. (e,f) Grain boundary distribution according to misorientation angle. Results for the cross section along the wire axis (left column) and perpendicular to the wire axis (right column)

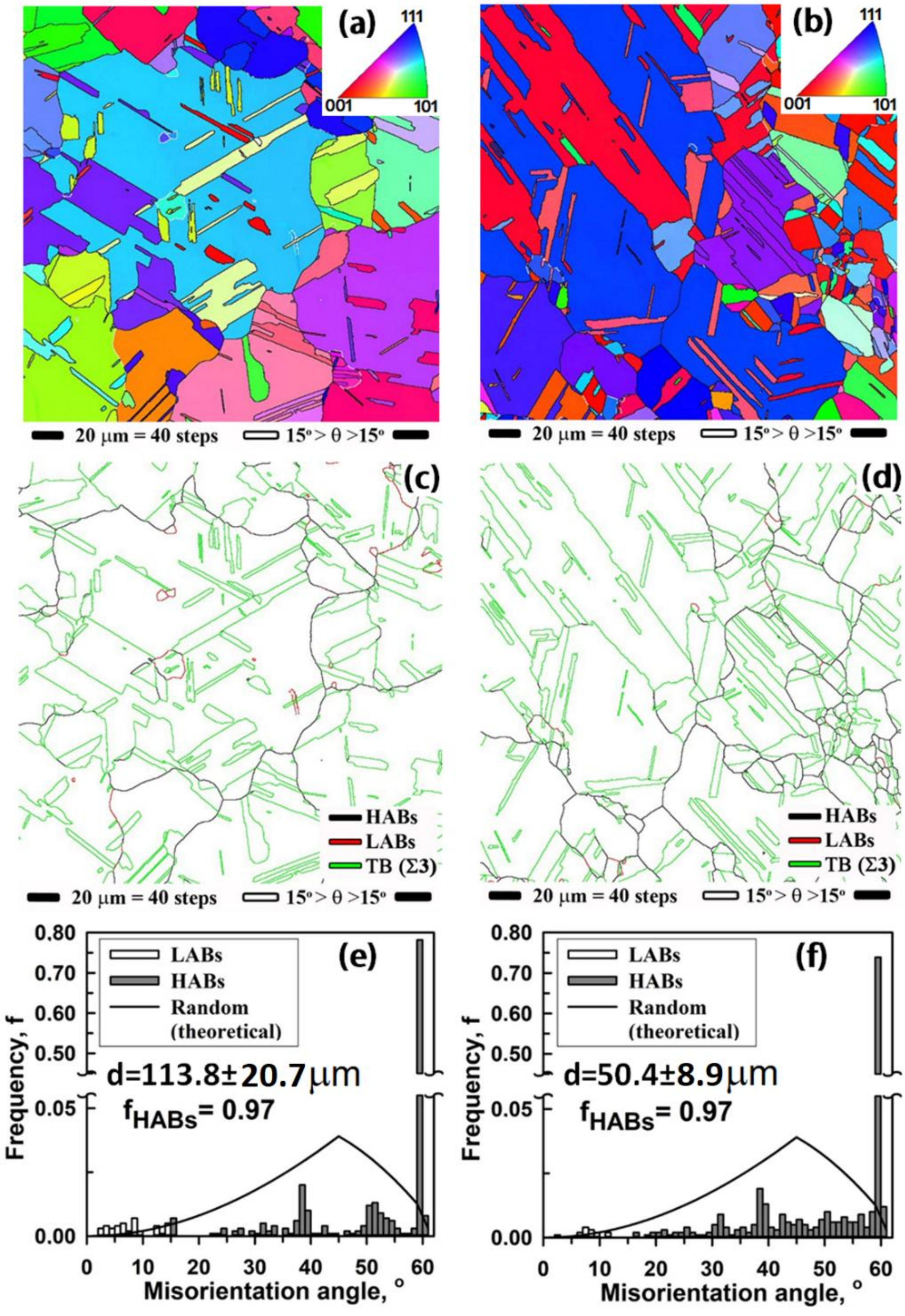

Fig. 2. Same as in Figure 1, but for annealed copper wire

2.2Stress-Strain Curves

Mechanical tensile tests to obtain the stress-strain curves are performed on specimens with gauge length L_0 = 10 mm at room temperature on an IM5081 horizontal tensile testing machine. The results are presented in Figure 3. In (a), the stress-strain curves are compared for the as-received (green curve) and annealed (black curve) wires for the strain rate of 1.1×10^{-3} s^{-1}. In (b), the stress-strain curves for the annealed wire are presented for the strain rates 1.1×10^{-3} s^{-1}, 4.6 $\times10^{-3}$ s^{-1} and 9.7 $\times10^{-3}$ s^{-1}.

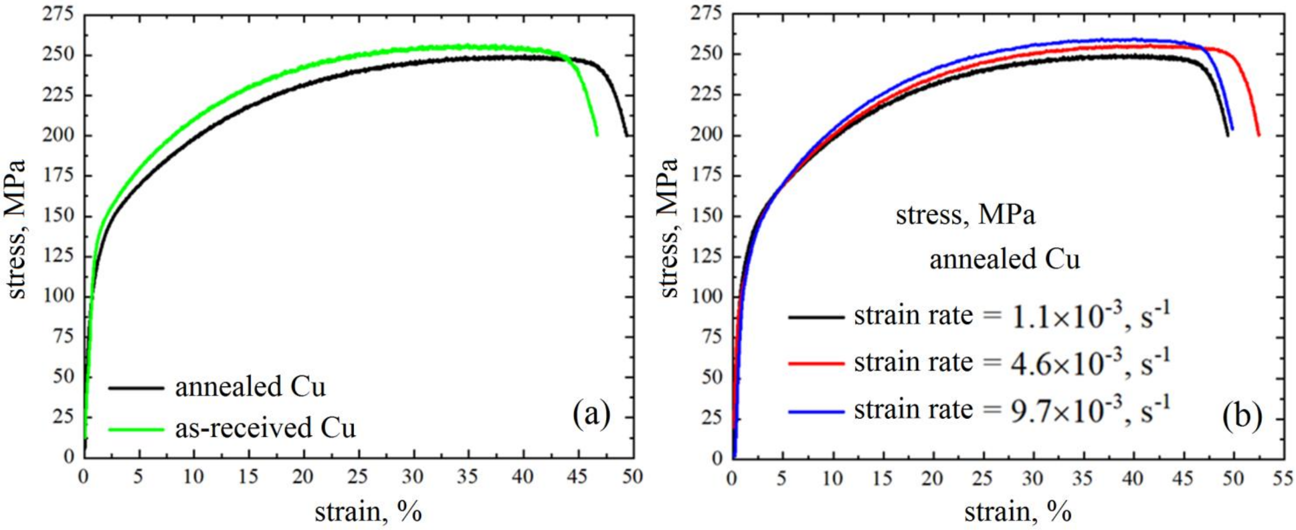

Fig. 3. (a) Stress-strain curves for as-received (green curve) and annealed (black curve) samples deformed at a strain rate of 1.1×10^{-3} s^{-1}. (b) The effect of the strain rate on the stress-strain curves for the annealed samples

It can be seen from Figure 3(a) that the annealed specimen deforms plastically at slightly lower stresses than the as-received specimen. Analysis of the elastic deformation stage has shown that the annealed (as-received) wire has a yield stress of σ_y=95 MPa (125 MPa). Figure 3(b) shows that the strain rate in the considered range does not have a strong influence on the plastic behavior of the specimens in tension. Only a slight increase in yield stress is observed with increasing strain rate.

2.3 Experimental Setup

To study the effect of electrical pulses on the plastic deformation of wires, an experimental setup was developed and assembled, see Figure 4. The wire sample (1) is mechanically loaded by a suspension (2) carrying loads of different masses (3). The strain of the sample is controlled by a dial micrometer (4). The specimen (1) is connected to the electrical unit (5) by means of conductors (6) with a large cross section. The voltage on the battery of capacitors of the electrical unit (5) is monitored by a digital voltmeter (7). The temperature of the sample is controlled by a pyrometer (8). The current through the sample is recorded by a current transformer (9) enclosed in a shield, the response of which is fed to channel 1 of an AKIP-4115/3A digital oscilloscope (10). The voltage drop across the sample is fed through a divider to channel 2 of the same oscilloscope. The change in voltage over time on the battery of capacitors as they are discharged through the sample is recorded using an oscilloscope USB attachment (11) connected to a portable personal computer (12).

The electrical circuit of the experimental setup is shown in Figure 5. An adjustable constant voltage source for charging a battery of capacitors is constructed from a laboratory autotransformer and a voltage doubler according to the simplest Latour-Delon-Grenachere circuit. The switch S1 is used to turn off the charging when the charge level required for the experiment is reached, which is visually controlled by a voltmeter to measure the voltage level and thus the charge of the battery of capacitors.

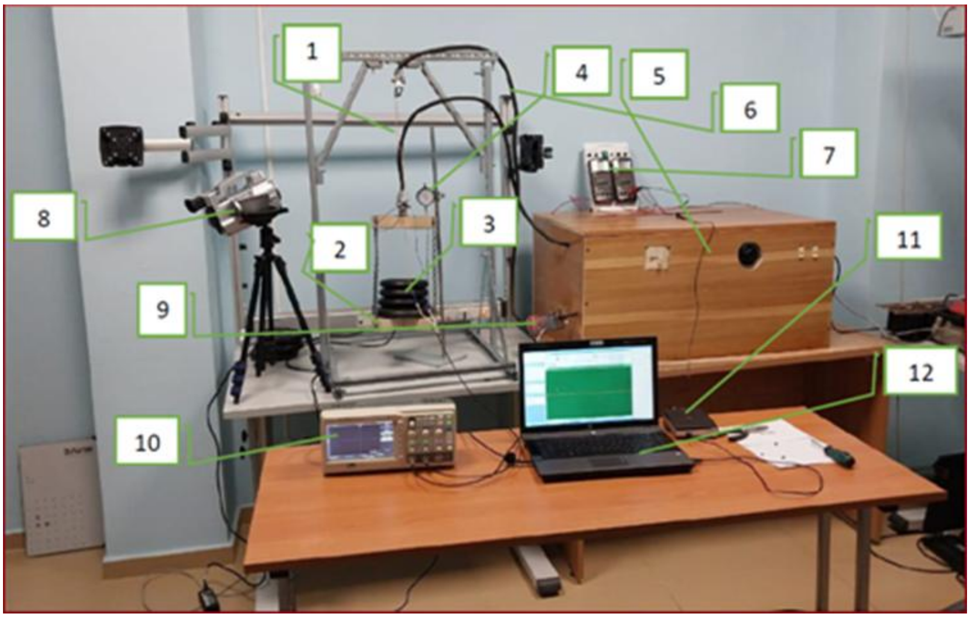

Fig. 4. Photo of the experimental setup for electroplasticity research

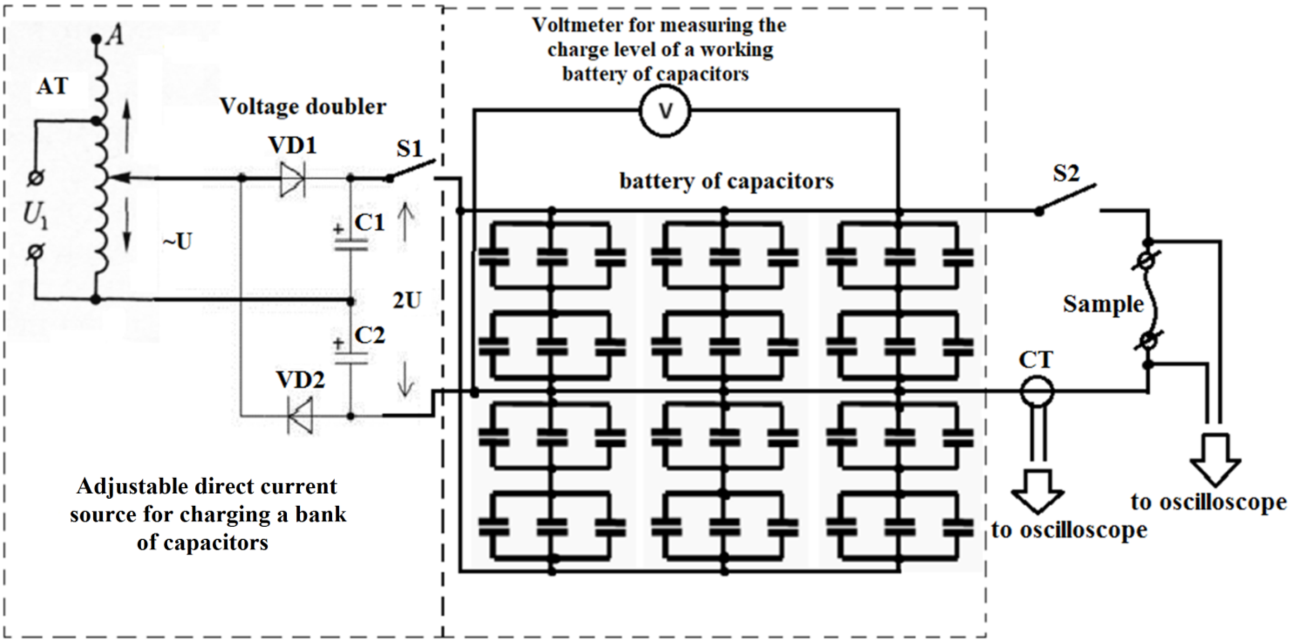

Fig. 5. Electrical circuit of the experimental setup

To perform an experiment on the effect of pulsed current on the plastic deformation of copper wire, the latter is loaded by the dead load up to the desired tensile stress. All experiments are performed at room temperature. After charging the battery of capacitors to the required voltage and turning off switch S1, the battery is discharged through the sample by turning on switch S2. The battery includes 36 electrolytic capacitors with a capacitance of 3300 µF and an operating voltage of up to 400 V each. The total capacitance of the battery of capacitors is C=29700 µF. In the conducted experiments the battery of capacitors is charged up to a voltage V=60 V. The choice of the charging voltage will be rationalized later. Total electrical energy stored in the battery is

$$W = \frac{CV^2}{2} = 53.5\,J. \tag{1}$$

The voltage drop across the sample and the current through the sample are monitored simultaneously. The current is recorded by a current transformer (CT) whose response is fed to the input of the oscilloscope, and the voltage drop across the sample is fed through a divider to another input of the oscilloscope. The current transformer is made of a ferrite ring of grade 2000NM1 with standard dimensions K45.0x28.0x12 on which 140 turns of wire of grade PEV-1 with a cross-sectional diameter of 0.5 mm are wound. To eliminate the impact of the current pulse on the current transformer, it is enclosed in a shielding shell. An example of the dependence of the current passing through the sample on time is given in Figure 6. From this graph one can see that the duration of the current pulse is about 0.1 ms and the maximum current density is 800 A/mm^2.

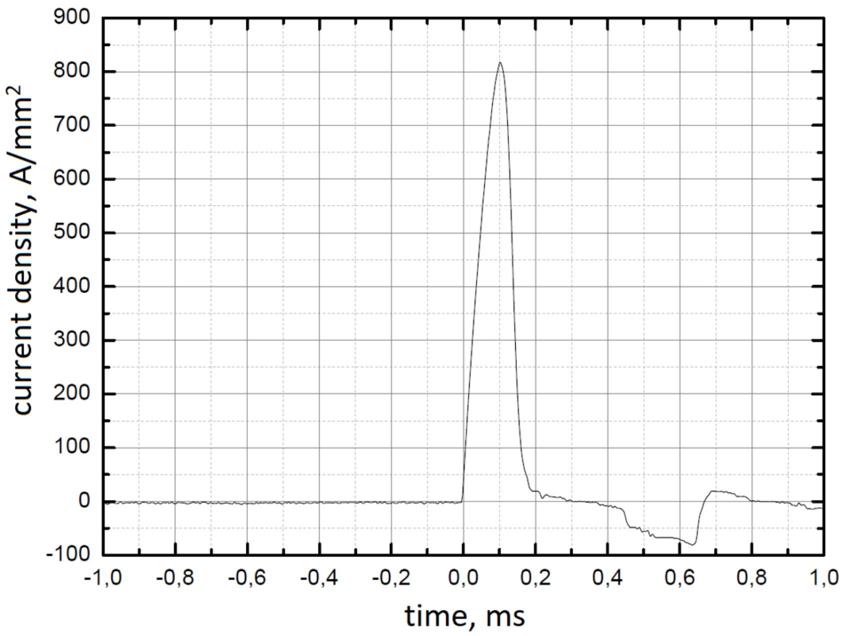

Fig. 6. An example of the dependence of the current through the sample as a function of time. This pulse is produced by discharging the battery of capacitors charged up to a voltage 60 V

This study investigates the effect of repetitive electrical pulses on the elongation of copper wire under dead load. A series of pulses is applied to the copper wire at a fixed tensile load, then the load is increased and a new series of pulses is applied, and so on. The increase in tensile strain of the wire, $\Delta\varepsilon$, is measured after each pulse. The time between pulses is approximately 15 seconds, which is necessary to ensure that the wire has cooled to room temperature after the Joule heat release from the current pulse.

3. Results

3.1 Joule Heat Release

First, it is instructive to measure the heat dissipation in the wires due to the current pulses. The copper wire was subjected to a tensile load of 80 MPa, which is within the elastic range. A capacitor battery was charged to a voltage V and discharged through the wire. The increment of tensile strain $\Delta\varepsilon$ was measured immediately after the electric pulse. This strain is due to the Joule heating of the wire and disappeared in a dozen of seconds as the wire cooled down in the air. The temperature increase of the wire is estimated from the thermal expansion formula,

$$\Delta T = \frac{\Delta\varepsilon_J}{\alpha}, \tag{2}$$

where α=16.9×10^{-6} K^{-1} is the coefficient of thermal expansion of copper at room temperature.

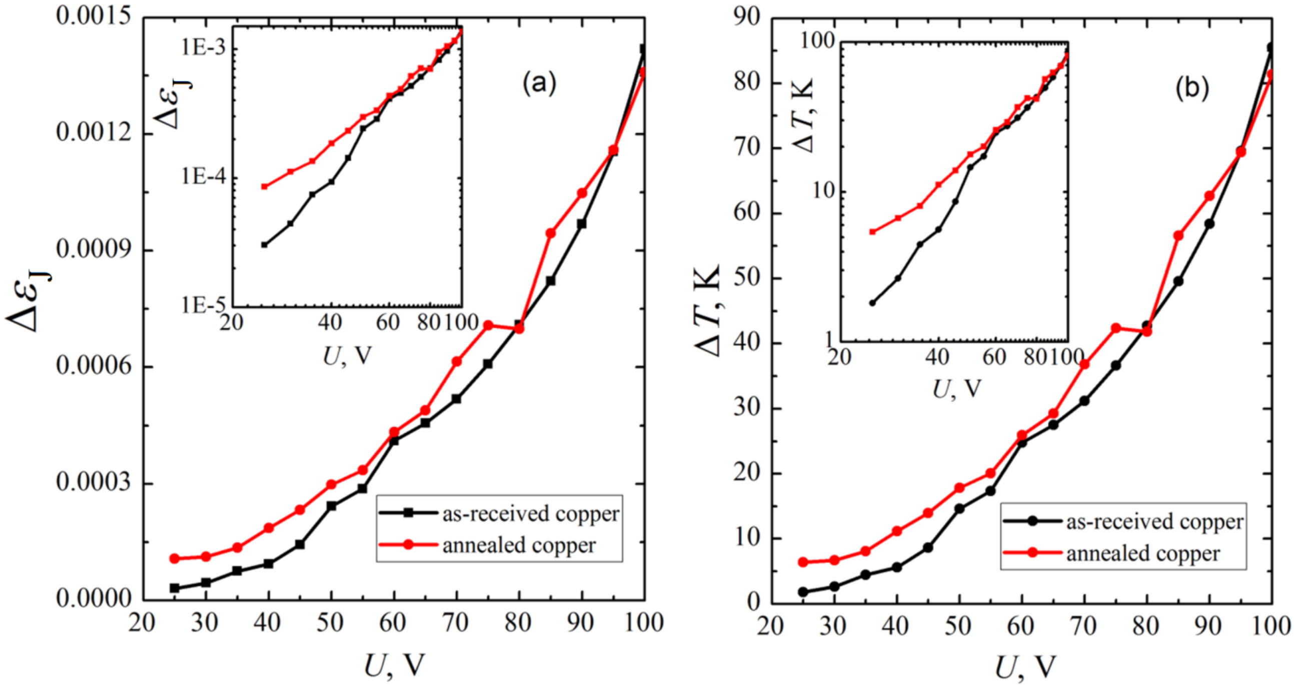

Fig. 7. (a) Increment of tensile strain of the wire due to electric pulse and (b) the corresponding increase in temperature of the wire as a function of the voltage of the capacitor battery discharged on the wire. The results for the as-received and annealed wires are shown in black and red, respectively. The insets show the results in log-log scale. The wires are under a tensile load of 80 MPa, which is within the elastic range, so the plastic deformation of the wires is zero.

The result is presented in Figure 7 for as-received (black) and annealed (red) wires. In (a) and (b), the increase in strain caused by the electrical pulse and the corresponding increase in temperature are shown as functions of the voltage on the capacitor. Insets show the curves in the log-log scale revealing the power dependence of $\Delta\varepsilon_J$ and ΔT on V,

$$\Delta\varepsilon_J \sim V^p, \qquad \Delta T \sim V^s\ . \tag{3}$$

The exponents s and p are greater for the as-received specimen than for the annealed specimen because the slope of the lines approximating the data in the log-log scale is greater for the as-received specimens. In particular, s=2.1 and 2.8 for the annealed and as-received specimens, respectively. The heat release increases faster with V for the as-received specimen because it contains more defects that are the centers of electron scattering.

As mentioned above, the experiments on the electroplasticity effect are carried out for the voltage on the capacitor battery of V=60 V. In this case, as shown in Figure 7(b), the temperature increase of the specimens, both in the as-received and in the annealed state, is about 25 K, which is insignificant and can be neglected.

Note that the strain increment of the wire due to the Joule heating is $\Delta\varepsilon_J$=4.0×10^{-4} for the as-received specimen and $\Delta\varepsilon_J$=4.4×10^{-4} for the annealed specimen. This strain due to the Joule heating is subtracted from the total strain of the wire $\Delta\varepsilon$ to find the plastic strain caused by the electric pulse:

$$\Delta\varepsilon_p = \Delta\varepsilon - \Delta\varepsilon_J\ . \tag{4}$$

3.2 Wire Elongation Under the Action of Repeated Electric Pulses

In the first set of experiments 15 current pulses are applied for each tensile stress and then the stress is increased. The increment of the plastic tensile strain of the wire, $\Delta\varepsilon_p$, calculated according to Eq. (4), is presented in Figure 8 as the function of the pulse number for the seven values of tensile stress. In (a) and (b) the results for the as-received and annealed specimens are shown.

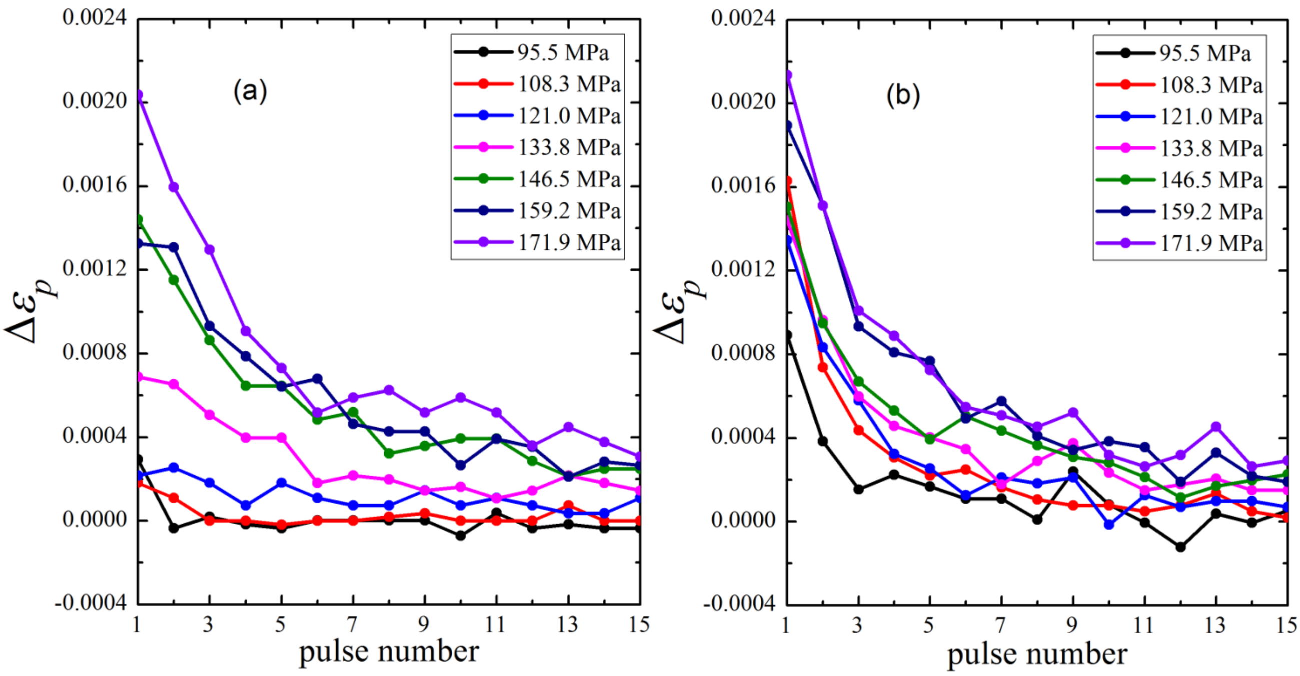

Fig. 8. Increment of plastic tensile strain as a function of the electric pulse number at seven values of fixed tensile stress, as indicated in the legends. Fifteen current pulses are applied at each tensile stress and then the load is increased. Results for (a) as-received specimen and (b) annealed specimen

As follows from the results presented in Figure 8(a), at tensile stresses in the range of 95.5-121 MPa acting on the specimen in the as-received state, the electroplastic effect is practically not manifested (black, red and blue curves). The observed strain increment of $\Delta\varepsilon$=$\Delta\varepsilon_J$ is a fully reversible strain associated with thermal expansion of the wire due to the released Joule heat. After passing the current pulse, the sample elongates, but during about 15 seconds while the electric block is charging, it cools down and the strain disappears. Note that the absence of the electroplastic effect in the indicated range of tensile stresses is due to the fact that these stresses are less than the yield stress of the copper wire in the delivery state (σ_y=125 MPa).In the case of tensile stresses above σ_y, the electroplastic effect begins to manifest itself in the fact that when current pulses are passed, the sample elongates by an amount greater than the thermal expansion strain, and after cooling down, residual plastic deformation is observed. It can be seen that the greater the tensile stress, the greater the elongation of the specimen. However, with each subsequent pulse, the electroplastic effect weakens, which is expressed by a decrease in strain increment $\Delta\varepsilon$ with pulse number. This is apparently due to the fact that dislocations, whose motion is activated by electric current pulses, gradually reach new more strong obstacles, so that plastic deformation at a given level of tensile stress and a given power of the current pulse no longer occurs.

Similar results for the annealed specimen are shown in Figure 8(b). It can be observed that the electroplastic effect is manifested here at lower tensile stresses compared to the unannealed specimen because the yield strength is lower for the former (σ_Y=95 MPa). The elongation occurring during the first current pulse at the same tensile stresses is slightly higher compared to the specimen in the as-received condition, which can be explained by the higher mobility of the dislocations. However, the electroplastic effect for annealed specimens decays faster with the number of pulses. This is due to the fact that after annealing, the density of dislocations required to realize plastic deformation becomes smaller.

In the second experiment, the tensile stress was incrementally increased by approximately 5% after four current pulses were applied at the same tensile stress. The results over the tensile stress range of 83 to 191 MPa are shown in Figure 9 for (a) the as-received specimen and (b) the annealed specimen. The four curves show the increment of plastic tensile strain of the specimen after each of the four pulses applied at a fixed value of tensile stress. For pulses one through four, the curves are shown in black, red, blue, and magenta, respectively.

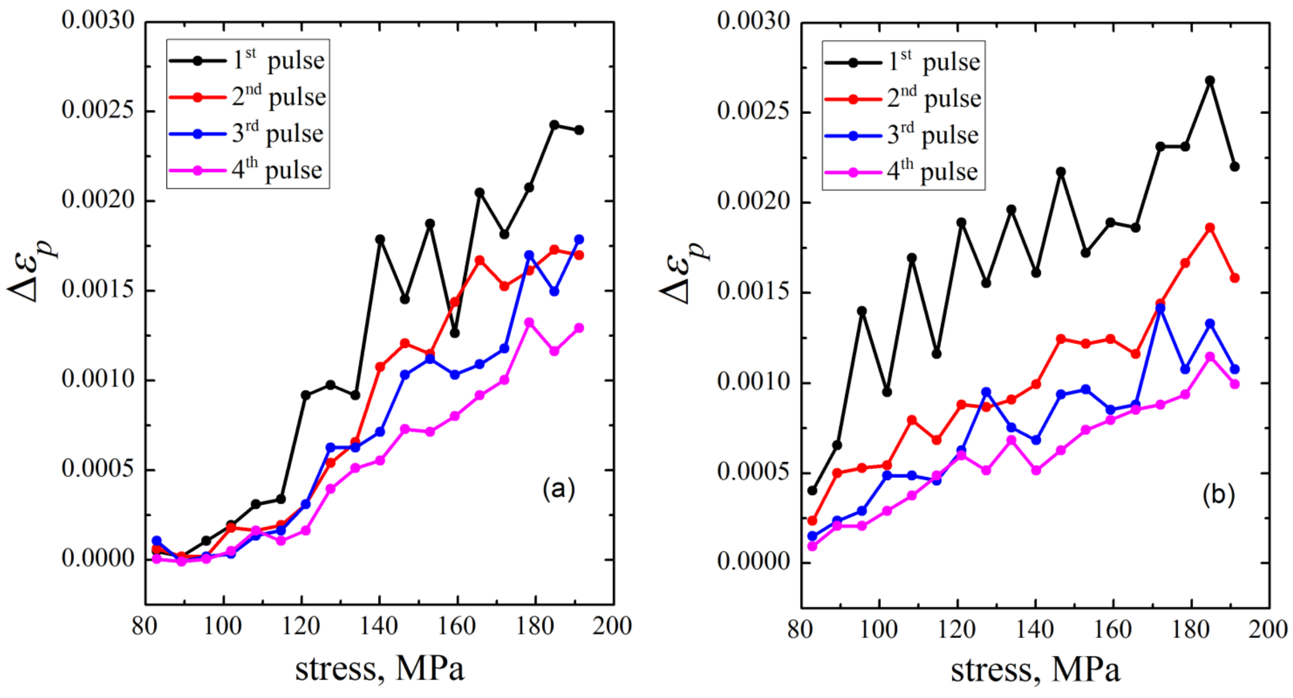

Fig. 9. Dependence of the plastic tensile strain increment on the stress for each of the four pulses applied at a fixed stress: (a) as-received sample and (b) annealed sample

It can be seen that regardless of the structural state of the copper, the strain increment increases with increasing tensile stress for all four pulses. At the same time, the dependence found in the previous stage of the experiment is maintained, i.e. each subsequent pulse gives a smaller strain of the wire. This is most evident in the case of the annealed specimen shown in Figure 9(b), where the strain increase after the first pulse is significantly higher compared to the subsequent pulses. It can also be observed that for the specimens in the as-received condition shown in Figure 9(a), the electroplastic effect takes place at tensile stresses slightly below the yield stress, starting at 120 MPa. This can be explained by the fact that the electroplastic effect reduces the yield strength.

3.3 Heat Release due to Plastic Deformation

The experimental setup used in this study (dead load loading) allows the heat release due to plastic deformation of the wire to be estimated and compared to the Joule heat release. The plastic deformation of the wire causes the dead load of the mass M to move downwards by ΔL. The work done by the weight on this displacement, $\Delta A = Mg\Delta L$, where g is the acceleration of free fall, is assumed to be entirely spent to increase the internal energy of the wire ΔE in the form of heat, then the temperature increase of the wire is

$$\Delta T = \frac{\Delta E}{cm} = \frac{\Delta A}{cm} = \frac{Mg\Delta L}{cm}, \qquad (5)$$

where c=390 J/(kg·K) is the specific heat capacity of copper and $m=2.56\times10^{-3}$ kg is the mass of the specimen.

The irreversible elongation of the wire is $\Delta L = L\Delta\varepsilon_p$, where L=0.36 m is the length of the wire. Tensile stress applied to the wire is $\sigma = Mg/S$, where $S=7.85\times10^{-7}$ m^2 is the cross section area of the wire. In view of this, Eq. (5) obtains the form

$$\Delta T = \frac{\sigma S L \Delta\varepsilon_p}{cm}. \qquad (6)$$

For example, referring to Figure 9(b), for σ=180 MPa one has $\Delta\varepsilon_p=2.3\times10^{-3}$ after the first pulse, and from Eq. (6) the increase in temperature is ΔT=0.117 K. This is two orders of magnitude smaller than the Joule heat release (25 K).

4. Discussion and Conclusions

The effect of pulsed electric current on the plastic deformation of M1 grade copper wires was investigated. An experimental setup was developed to analyze the effect of repetitive current pulses at a fixed tensile stress produced by a dead load, see Figure 4.

The use of specimens with a relatively large gauge length (360 mm) allowed the strain increments of the wires produced by the electrical pulses to be measured with high accuracy using a dial micrometer. In particular, it was possible to measure the thermal expansion of the wires loaded in the elastic region and, using the thermal expansion formula Eq. (2), to calculate the temperature increase of the wire, see Figure 5. It was found that for the wire loaded in the elastic region, the temperature increase due to Joule heat is a power function of the voltage on the capacitor battery, $\Delta T \sim V^s$, and the exponent s=2.1 and 2.8 for the annealed and as-received specimens, respectively. The fact that s is smaller for the annealed copper is explained by the lower density of dislocations and grain boundaries, which are the main centers of electron scattering and heat release. Interestingly, $s>2$ for both samples, but the electrical energy stored by the capacitor battery is proportional to V^2, see Eq. (1). This means that the Joule heat release increases faster with increasing V than the energy stored in the capacitor. This is the effect of nonlinearity in the interaction of electrons with the defects.

Based on the results shown in Figure 5(b), the voltage at the capacitor battery of 60 V was chosen for the experiments. At this voltage, the temperature increase of the wires is about 25 K, which is rather small, and the observed plastic deformation is due to the interaction of electrons with the lattice defects and cannot be explained by Joule heating. It was also found that at the voltage of 60 V, the thermal expansion of the wires causes the strain $\Delta\varepsilon_J$=4.0×10^{-4} for the as-received specimen and $\Delta\varepsilon_J$=4.4×10^{-4} for the annealed specimen. This strain due to Joule heating was subtracted from the total strain of the wire according to Eq. (4) in order to find the increment of plastic strain $\Delta\varepsilon_p$.

The experimental setup used in this study makes it possible to solve another problem that can hardly be solved by other experimental methods. This is the evaluation of heat generation due to plastic deformation induced by an electric pulse, see Section 3.3. This evaluation is carried out under the assumption that the work done by the dead load in the displacement caused by the plastic deformation of the wire is completely converted into thermal energy of the wire. The calculated temperature increment was found to be two orders of magnitude smaller than the heating due to Joule heat release. However, it should be noted that the energy associated with plastic deformation is released in a small volume around the moving dislocation cores, and its consideration may be important for understanding the mechanisms of electroplastic deformation. This heat release may further stimulate dislocation sliding in addition to the heat released by electron scattering on dislocations.

Our main finding is that the increase in plastic strain of the wire at fixed tensile stress decreases with the number of electrical pulses, see Figures 8 and 9. The following physical interpretation of this fact can be offered. At a given stress, dislocations are pinned to the obstacles. An electric pulse causes the non-homogeneous heat release mainly at the dislocation cores, since they are efficient electron scatterers. The local temperature increase around the dislocations increases their mobility. The dislocations start to slip and move to a colder region of the crystal lattice where they stop. The movement of the dislocations produces an increase in plastic deformation. Successive electric pulses at fixed stress result in dislocation motion and their pinning to even stronger obstacles, that is why the increment of plastic strain decreases with the number of electric pulses. Similar effect of reduction of the plastic strain increment under successive electric pulses has been observed in the work [56] for electric pulse assisted nanoindentation and macroscopic compression.

Overall, the presented results confirm that a noticeable increase in plastic deformation of the specimens occurs at a very small net temperature increase (25 K in our experiments). The effect of electroplasticity can be used to develop an energy-saving method of metal forming, since the energy of the electric pulses is mainly spent on heating the dislocations rather than the bulk of the crystal, and the dislocation motion produces the desired plastic deformation. In future studies, the effect of electroplasticity will be analyzed for other metals, such as aluminum, which has a very different stacking fault energy than copper and therefore a different dislocation behavior.

Author Contributions
Conceptualization, S.V.D., O.B.N, A.V.Kh. and V.V.S.; methodology, P.S.T., V.P.T. and A.S.S.; investigation, A.Y.M., D.V.T., G.R.Kh. and D.U.A.; data curation, A.Y.M., D.V.T., G.R.Kh. and D.U.A.; writing—original draft preparation, S.V.D. and A.Y.M. All authors have read and agreed to the published version of the manuscript.

Funding

For S.V.D. this research was funded by the Russian Science Foundation, grant number 24-11-00139 (conceptualization, writing—original draft preparation). The work of A.Y.M. and D.V.T. was supported by the Ministry of Science and Higher Education of the Russian Federation within the framework of the state task of the Ufa University of Science and Technologies (No. 075- 03-2024-123/1) of the youth research laboratory "Metals and Alloys under Extreme Impacts" (investigation, data curation).

Data Availability Statement

The data that support the findings of this study are available on request from the corresponding author, S.V.D.

Conflicts of Interest

The authors declare that they have no known competing financial interests or personal relationships that could have appeared to influence the work reported in this paper.

Acknowledgement

This research was funded by the Russian Science Foundation, grant number 24-11-00139.

References

[1] Troitskii, O. A. (1969) Electromechanical effect in metals. *JETP Letters*, 1, 18–22. http://jetpletters.ru/ps/0/article_25672.shtml

[2] Okazaki, K., Kagawa, M., & Conrad, H. (1978). A study of the electroplastic effect in metals. *Scripta Metallurgica*, 12(11), 1063-1068. https://doi.org/10.1016/0036-9748(78)90026-1

[3] Stolyarov, V., & Misochenko, A. (2023). A pulsed current application to the deformation processing of materials. *Materials*, 16(18), art. no. 6270. https://doi.org/10.3390/ma16186270

[4] Izadpanah, S., Cao, X., An, D., Li, X., & Chen, J. (2023). One step forward to electrically assisted forming mechanisms and computer simulation: A review. *Advanced Engineering Materials*, 25(5), art. no. 2200425. https://doi.org/10.1002/adem.202200425

[5] Dong, H.-R., Li, X.-Q., Li Y., Wang, Y.-H., Wang, H.-B., Peng, X.-Y., & Li, D.-S. (2022). A review of electrically assisted heat treatment and forming of aluminum alloy sheet. *International Journal of Advanced Manufacturing Technology*, 120 (11-12), 7079 – 7099. https://doi.org/10.1007/s00170-022-08996-6

[6] Ding, J., Li H., Bian, T., & Ma, J. (2018). Electroplasticity and electrically-assisted forming: A critical review. *Hangkong Xuebao/Acta Aeronautica et Astronautica Sinica*, 39(1), art. no. 021201. https://doi.org/10.7527/S1000-6893.2017.021201

[7] Grimm, T. J., & Mears, L. M. (2022). Skin effects in electrically assisted manufacturing. *Manufacturing Letters*, 34, 67 – 70. https://doi.org/10.1016/j.mfglet.2022.09.006

[8] Zhan, L., Li, R., Wang, J., Xue, X., Wang, Y., & Lv, Z. (2023). Thermoelectric coupling deep drawing process of ZK60 magnesium alloys. *International Journal of Advanced Manufacturing Technology*, 126(7-8), 3005 – 3014. https://doi.org/10.1007/s00170-023-11300-9

[9] Lv, Z., Zhou, Y., Zhan, L., Zang, Z., Zhou, B., & Qin, S. (2021). Electrically assisted deep drawing on high-strength steel sheet. *International Journal of Advanced Manufacturing Technology*, 112(3-4), 763 – 773. https://doi.org/10.1007/s00170-020-06335-1

[10] Qian, L., Zhan, L., Zhou, B., Zhang, X., Liu, S., & Lv, Z. (2021). Effects of electroplastic rolling on mechanical properties and microstructure of low-carbon martensitic steel. *Materials Science and Engineering: A*, 812, 141144. https://doi.org/10.1016/j.msea.2021.141144

[11] Pochivalov Yu, I. (2023). Structure and properties of low-alloy steel 10G2FBYu after rolling in embossed rolls under conditions of electroplasticity. *Izvestiya Ferrous Metallurgy*, 66(6), 659 – 665. https://doi.org/10.17073/0368-0797-2023-6-659-665

[12] Li, C., Xu, Z., Peng, L., & Lai, X. (2022). An electric-pulse-assisted stamping process towards springback suppression and precision fabrication of micro channels. *International Journal of Mechanical Sciences*, 218, 107081. https://doi.org/10.1016/j.ijmecsci.2022.107081

[13] Perkins, T. A., Kronenberger, T. J., & Roth, J. T. (2007). Metallic forging using electrical flow as an alternative to warm/hot working. *Journal of Manufacturing Science and Engineering*, 129(1), 84–94. https://doi.org/10.1115/1.2386164
[14] Perkins, T. A., & Roth, J. T. (2005). The reduction of deformation energy and increase in workability of metals through an applied electric current. *American Society of Mechanical Engineers, Manufacturing Engineering Division, MED*, 16-1, 313 – 322. https://doi.org/10.1115/IMECE2005-81060
[15] Zhao, L., Chen, G., Liu, J., Wei, H., & Huang, J. (2024). Effect of pulse current parameters on electroplastically assisted dry cutting performance of W93NiFe alloy. *International Journal of Advanced Manufacturing Technology*, 131(5-6), 2123 – 2131. https://doi.org/10.1007/s00170-022-10762-7
[16] Dong, H., Li, X., Li, Y., Zhao, S., Wang, H., Liu, X., Meng, B., & Du, K. (2023). The anomalous negative electric current sensitivity of a precipitation hardened Al alloy during electrically-assisted forming. *Journal of Materials Research and Technology*, 24, 9356 – 9368. https://doi.org/10.1016/j.jmrt.2023.05.161
[17] Xu, Z., Jiang, T., Huang, J., Peng, L., Lai, X., & Fu, M. W. (2022). Electroplasticity in electrically-assisted forming: Process phenomena, performances and modeling. *International Journal of Machine Tools and Manufacture*, 175, 103871. https://doi.org/10.1016/j.ijmachtools.2022.103871
[18] Tiwari, J., Prasad, K., Krishnaswamy, H., & Amirthalingam, M. (2023). Energy density to explain the ductility loss during electroplastic deformation of a dual phase steel. *Materials Characterization*, 205, 113359. https://doi.org/10.1016/j.matchar.2023.113359
[19] Abdullina, D. U., Bebikhov, Yu. V., Tatarinov, P. S. & Dmitriev, S. V. (2023). Review of recent achievements in the field of electroplastic metal forming. *Basic Problems of Material Science*, 20(4), 469‑483. https://doi.org/10.25712/ASTU.1811-1416.2023.04.006
[20] Dimitrov, N., Liu, Yu., & Horstemeyer, M. (2020). Electroplasticity: A review of mechanisms in electro-mechanical coupling of ductile metals. *Mechanics of Advanced Materials and Structures*, 29, 1-12. https://doi.org/10.1080/15376494.2020.1789925
[21] Kim, M.-J., Yoon, S., Park, S., Jeong, H.-J., Park, J.-W., Kim, K., Jo, J., Heo, T., Hong, S.-T., Cho, S.H., Kwon, Y.-K., Choi, I.-S., Kim, M., & Han, H. N. (2020). Elucidating the origin of electroplasticity in metallic materials. *Applied Materials Today*, 21, 100874. https://doi.org/10.1016/j.apmt.2020.100874
[22] Li, X., Zhu, Q., Hong, Y., Zheng, H., Wang, J., Wang, J., & Zhang, Z. (2022). Revealing the pulse-induced electroplasticity by decoupling electron wind force. *Nature Communications*, 13(1), 6503. https://doi.org/10.1038/s41467-022-34333-2
[23] Krishnaswamy, H., Tiwari, J., & Amirthalingam, M. (2024). Revisiting electron-wind effect for electroplasticity: A critical interpretation. *Vacuum*, 221, 112937. https://doi.org/10.1016/j.vacuum.2023.112937
[24] Li, H., Jin, F., Zhang, M., Ding, J., Bian, T., Li, J., Ma, J., Zhang, L., & Wang, Y. (2023). Decoupling electroplasticity by temporal coordination design of pulse current loading and straining. *Materials Science and Engineering: A*, 881, 145435. https://doi.org/10.1016/j.msea.2023.145435
[25] Dimitrov, N.K., Liu, Y., & Horstemeyer, M.F. (2022). Electroplasticity: A review of mechanisms in electro-mechanical coupling of ductile metals. *Mechanics of Advanced Materials and Structures*, 29(5), 705 – 716. https://doi.org/10.1080/15376494.2020.1789925
[26] Hao, S., Chu, Q., Li, W., Yang, X., & Zou, Y. (2023). Effect of electropulsing treatment on the microstructure and mechanical properties of metallic materials: a review. *Cailiao Daobao/Materials Reports*, 37(4), 21030039. https://doi.org/10.11896/cldb.21030039
[27] Liu, J., Jia, D., Fu, Y., Kong, X., Lv, Z., Zeng, E., & Gao, Q. (2024). Electroplasticity effects: from mechanism to application. *International Journal of Advanced Manufacturing Technology*, 131(5-6), 3267–3286. https://doi.org/10.1007/s00170-023-12072-y
[28] Jeong, H.-J., Kim, M.-J., Choi, S.-J., Park, J.-W., Choi, H., Luu, V. T., Hong, S.-T., & Han, H. N. (2020). Microstructure reset-based self-healing method using sub-second electric pulsing for metallic materials. *Applied Materials Today*, 20, 100755. https://doi.org/10.1016/j.apmt.2020.100755
[29] Kim, M.-J., Lee, M.-G., Krishnaswamy, H., Hong, S.-T., Choi, I.-S., Kim, D., Oh, K. H., & Han, H. (2016). Electric current–assisted deformation behavior of Al-Mg-Si alloy under uniaxial tension. *International Journal of Plasticity*, 94, 148-170. https://doi.org/10.1016/j.ijplas.2016.09.010
[30] Wang, X., Zhou, B., Huang, H., Niu, J., Guan, S., & Yuan, G. (2022). Extraordinary ductility enhancement of Mg-Nd-Zn-Zr alloy achieved by electropulsing treatment. *Journal of Magnesium and Alloys.* https://doi.org/10.1016/j.jma.2022.07.007
[31] Dobras, D., Zimniak, Z., Zwierzchowski, M., & Dziubek, M. (2024). Effect of strain rate on the mechanical behavior of Al-Mg alloy under a pulsed electric current. *Metallurgical and Materials Transactions A,* 55, 1284–1294. https://doi.org/10.1007/s11661-024-07335-6

[32] Herbst, S., Karsten, E., Gerstein, G., Reschka, S., Nürnberger, F., Zaefferer, S., & Maier, H.J. (2023). Electroplasticity mechanisms in hcp materials. *Advanced Engineering Materials*, 25(18), 2201912. https://doi.org/10.1002/adem.202201912

[33] Yin, F., Ma, S., Hu, S., Liu, Y., Hua, L., & Cheng, G. J. (2023). Understanding the microstructure evolution and mechanical behavior of titanium alloy during electrically assisted plastic deformation process. *Materials Science and Engineering: A*, 869, 144815. https://doi.org/10.1016/j.msea.2023.144815

[34] Tiwari, J., Pratheesh, P., Bembalge, O.B., Krishnaswamy, H., Amirthalingam, M., & Panigrahi, S. K. (2021). Microstructure dependent electroplastic effect in AA 6063 alloy and its nanocomposites. *Journal of Materials Research and Technology*, 12, 2185 – 2204. https://doi.org/10.1016/j.jmrt.2021.03.112

[35] Jeong, H.-J., Park, J.-W., Shin, E., Woo, W., Kim, M.-J., & Han, H. N. (2022). Electric current-induced precipitation hardening in advanced high-strength steel. *Scripta Materialia*, 220, 114933. https://doi.org/10.1016/j.scriptamat.2022.114933

[36] McNeff, P. S., & Paul, B. K. (2020). Electroplasticity effects in Haynes 230. *Journal of Alloys and Compounds*, 829, 154438. https://doi.org/10.1016/j.jallcom.2020.154438

[37] Dong, H., Zhou, H., Li, Y., Li, X., Zhao, S., Liu, X., & Wang, Y. (2024) Temperature-dependent electroplasticity in the Invar 36 alloy. *Journal of Materials Research and Technology*, 29, 3842–3848. https://doi.org/10.1016/j.jmrt.2024.02.125

[38] Chen, C., Li, C., Li, C., Li, F., Zhang, G., & Yu, G. (2022). Effect of angle between pulse current and load direction on flow stress of Ti-6Al-4V alloy under uniaxial tension. *Journal of Materials Engineering and Performance*, 31(11), 9283 – 9293. https://doi.org/10.1007/s11665-022-06921-2

[39] Yang, Z., Bao, J., Ding C., Son, S., Ning, Z., Xu, J., Shan, D., Guo, B., & Kim, H. S. (2023). Electroplasticity in the Al0.6CoCrFeNiMn high entropy alloy subjected to electrically-assisted uniaxial tension. *Journal of Materials Science and Technology*, 148, 209 – 221. https://doi.org/10.1016/j.jmst.2022.11.031

[40] Li, X., Hong, Y., Ke, H., Zhong, L., Zou, Y., & Wang, J. In situ TEM study of pulse-enhanced plasticity of monatomic metallic glasses (2024) Journal of Materials Science and Technology, 195, 208–217. https://doi.org/10.1016/j.jmst.2023.12.068

[41] Li, X., Turner, J., Bustillo, K., & Minor, A. M. (2022). In situ transmission electron microscopy investigation of electroplasticity in single crystal nickel. Acta Materialia, 223, 117461. https://doi.org/10.1016/j.actamat.2021.117461

[42] Kang, W., Beniam, I., & Qidwai, S. M. (2016). In situ electron microscopy studies of electromechanical behavior in metals at the nanoscale using a novel microdevice-based system. *Review of Scientific Instruments*, 87(9), 095001. https://doi.org/10.1063/1.4961663

[43] Zhou, C., Zhan, L., Li, H., Liu, C., Xu, Y., Ma, B., Yang, Y., & Huang, M. (2022). Dislocation reconfiguration during creep deformation of an Al-Cu-Li alloy via electropulsing. *Journal of Materials Science and Technology*, 130, 27–34. https://doi.org/10.1016/j.jmst.2022.05.008

[44] Zhao, S., Zhang, R., Chong, Y., Li, X., Abu-Odeh, A., Rothchild, E., Chrzan, D.C., Asta, M., Morris, J. W., Jr., & Minor, A. M. (2021). Defect reconfiguration in a Ti–Al alloy via electroplasticity. *Nature Materials*, 20(4), 468 – 472. https://doi.org/10.1038/s41563-020-00817-z

[45] Kumar, A., & Paul, S.K. (2020). Healing of fatigue crack in steel with the application of pulsed electric current. *Materialia*, 14, 100906. https://doi.org/10.1016/j.mtla.2020.100906

[46] Yoon, S., Gu, S., Li, S., Kimura, Y., Toku, Y., & Ju, Y. (2023). Efficiency improvement of fatigue crack healing by multiple high-density pulsed electric currents: Application to austenitic stainless steel. *Engineering Fracture Mechanics*, 284, 109235. https://doi.org/10.1016/j.engfracmech.2023.109235

[47] Zhao, Z., Li, X., Yuan, H., Zhao, Y., & Qi, J. (2023). Influence of pulse frequency on the wear and corrosion resistance of Al-4.5Mg-3Si alloy. *Journal of Materials Engineering and Performance*, 32(24), 11448 – 11456. https://doi.org/10.1007/s11665-023-07942-1

[48] Xue,, L., Liao C., Wu, M., Li, Q., Hu, Z., Yang, Y., & Liu, J. (2024). Improvement of mechanical properties and corrosion resistance of SLM-AlSi10Mg alloy by an eco-friendly electric pulse treatment. *Journal of Cleaner Production*, 439, 140864. https://doi.org/10.1016/j.jclepro.2024.140864

[49] Barimani-Varandi, A., & Jalali Aghchai, A. (2021). Enhancement of the tensile shear strength for joining low-ductility aluminium to high-strength steel by using electrically-assisted mechanical clinching (EAMC). *Proceedings of the Institution of Mechanical Engineers, Part B: Journal of Engineering Manufacture*, 235(11), 1790 – 1799. https://doi.org/10.1177/0954405421995652

[50] Xiao, X., Xu, S., Sui, D., & Zhang, H. (2021). The electroplastic effect on the deformation and twinning behavior of AZ31 foils during micro-bending tests. *Materials Letters*, 288, 129362. https://doi.org/10.1016/j.matlet.2021.129362

[51] Bao, J., Chen, W., Bai, J., Xu, J., Shan, D., & Guo, B. (2022). Local softening deformation and phase transformation induced by electric current in electrically-assisted micro-compression of Ti–6Al–4V alloy. *Materials Science and Engineering: A*, 831, 142262. https://doi.org/10.1016/j.msea.2021.142262

[52] Li, X., Xu, Z., Guo, P., Peng, L., & Lai, X. (2022). Electroplasticity mechanism study based on dislocation behavior of Al6061 in tensile process. *Journal of Alloys and Compounds*, 910, 164890. https://doi.org/10.1016/j.jallcom.2022.164890

[53] Li, P., Liu, L., Hu, L., Zhang, Y., Yan, S.-L., & Xue, K.-M. (2023). Flow softening rules and mechanisms in Ti–6Al–4V alloy sheet during electrically assisted near-isothermal tension. *Journal of Materials Science*, 58(4), 1925 – 1938. https://doi.org/10.1007/s10853-023-08140-z

[54] Cao, X., An, D., Liu, Q., Chen, G., & Li, X. (2024). Precipitation hardening characterization and stress prediction model in electrically-assisted Ti2AlNb uniaxial tension. *Intermetallics*, 167, 108214. https://doi.org/10.1016/j.intermet.2024.108214

[55] Wu, C., Zhou, Y.J., & Liu, B. (2022). Experimental and simulated investigation of the deformation behavior and microstructural evolution of Ti6554 titanium alloy during an electropulsing-assisted microtension process. *Materials Science and Engineering: A*, 838, 142745. https://doi.org/10.1016/j.msea.2022.142745

[56] Andre, D., Burlet, T., Körkemeyer F., Gerstein, G., Gibson, J. S. K.-L., Sandlöbes-Haut, S., & Korte-Kerzel, S. (2019). Investigation of the electroplastic effect using nanoindentation. *Materials and Design*, 183, 108153. https://doi.org/10.1016/j.matdes.2019.108153

[57] Omoigiade, O. (2018). Electric current as a steel wire manufacturing tool. *Materials Science and Technology*, 34(18), 2202 – 2213. https://doi.org/10.1080/02670836.2018.1488435

[58] Sánchez Egea, A. J., González Rojas, H. A., Celentano, D. J., & Jorba Peiró, J. (2016). Mechanical and metallurgical changes on 308L wires drawn by electropulses. *Materials and Design*, 90, 1159–1169. https://doi.org/10.1016/j.matdes.2015.11.067

[59] Humphreys, F. J. (2001). Review grain and subgrain characterization by electron back scatter diffraction. Journal of Materials Science, 36, 3833-3854. https://doi.org/10.1023/A:1017973432592